# New Concepts Relevant to Cisplatin Anticancer Activity from Unique Spectral Features Providing Evidence That Adjacent Guanines in d(GpG), Intrastrand-Cross-Linked at N7 by a *cis*-Platinum(II) Moiety, Can Adopt a Head-to-Tail Arrangement

**Luigi G. Marzilli,*,† Susan O. Ano,† Francesco P. Intini,‡ and Giovanni Natile,*,‡**

*Contribution from the Department of Chemistry, Emory University, Atlanta, Georgia 30322, and Dipartimento Farmaco-Chimico, Università degli Studi di Bari, 70125 Bari, Italy*

*Received May 17, 1999*

**Abstract:** N7−Pt−N7 d(GpG) intrastrand cross-link adducts are formed in DNA by the anticancer drug, cisplatin. By creating adducts with slow dynamic motion, we have identified a new abundant conformer with the guanine bases in a head-to-tail (HT) arrangement and with both sugars in the N pucker of A-form DNA instead of the S pucker of B-form DNA. Both features are unprecedented for such cross-links. The HT form is one of two abundant thermodynamic and kinetic products formed by addition of d(GpG) to [(*S*,*R*,*R*,*S*)-**Bip**Pt$(H_2O)_2]^{2+}$ (**Bip** = 2,2′-bipiperidine with *S*, *R*, *R*, and *S* configurations at the asymmetric N, C, C, and N chelate ring atoms). The second form has the common head-to-head conformation (HH1) with the backbone propagating in the normal direction, both G's *anti* and with N and S puckers for the 5′- and 3′-G residues, respectively. This form has a typical NMR shift pattern: upfield 5′-G H8, downfield 3′-G H8, and downfield $^{31}$P NMR signal. In contrast, the HT (*S*,*R*,*R*,*S*)-**Bip**Pt(d(GpG)) form has several unusual or unique NMR spectral features, including pronounced upfield shifts of *both* G H8 signals, unusually shifted 5′-G H3′ and 3′-G H2′ signals, and an unexpectedly upfield-shifted $^{31}$P NMR signal. A strong 3′-G H8−H1′ NOE cross-peak, the absence of an H8−H8 NOE cross-peak, and H1′ couplings establish that this form is an HT conformer with a *syn* 3′-G, an *anti* 5′-G, and *both* sugars having mainly N pucker. The HT base orientation in cross-links introduces chirality, and two conformers, ΔHT1 and ΛHT2, are possible with normal and opposite directions of backbone propagation, respectively. NMR-restrained molecular mechanics and dynamics calculations show that the ΔHT1 conformer has the lower energy. Of some interest, rules in the literature cannot account for the G H8 shifts of any **Bip**Pt(d(GpG)) form reported by us here and previously. We advance new rules that allow successful G H8 shift predictions for these cross-links and also for cisplatin oligonucleotide adducts; these rules are consistent with the solid-state structure of *cis*-Pt$(NH_3)_2$(d(pGpG)) (Sherman, S. E.; Gibson, D.; Wang, A. H.-J.; Lippard, S. J. *J. Am. Chem. Soc.* **1988**, *110*, 7368−7381), but they conflict with widely held interpretations of *cis*-Pt$(NH_3)_2$(d(GpG)) solution structure and dynamics. Finally, our results suggest that, in the future, the effect of the carrier ligands on the HH vs HT cross-link conformation must be considered in drug design.

## Introduction

Exceptional anticancer activity is displayed by cisplatin (*cis*-$PtCl_2(NH_3)_2$),[1] but its analogues [*cis*-$PtX_2A_2$: $A_2$ = a diamine or two amines; $X_2$ = anionic leaving ligand(s)] generally are less active.[2−7] An intrastrand DNA cross-link with Pt linking N7's of adjacent guanines (G) of DNA is the critical lesion accounting for activity (all G's mentioned here are platinated at N7).[2,5] The G bases in this cross-link are generally accepted to have the head-to-head (HH) orientation with two *anti* G's (HH1, Figure 1).[8−16] In virtually all reports on N7−Pt−N7 d(GpG) cross-links in both single-stranded and duplex adducts,

† Emory University.

‡ Università degli Studi di Bari.

(1) O'Dwyer, P. J.; Stevenson, J. P.; Johnson, S. W. In *Cisplatin: Chemistry and Biochemistry of a Leading Anticancer Drug*; Lippert, B., Ed.; Wiley-VCH: Weinheim, 1999; pp 31−69.

(2) Bloemink, M. J.; Reedijk, J. In *Metal Ions in Biological Systems, Vol. 32*; Sigel, H., Sigel, A., Eds.; Marcel Dekker: New York, 1996; Vol. 32, pp 641−685.

(3) Bloemink, M. J.; Engelking, H.; Karentzopoulos, S.; Krebs, B.; Reedijk, J. *Inorg. Chem.* **1996**, *35*, 619−627.

(4) Sundquist, W. I.; Lippard, S. J. *Coord. Chem. Rev.* **1990**, *100*, 293−322.

(5) Reedijk, J. *J. Chem. Soc., Chem. Commun.* **1996**, 801−806.

(6) Hambley, T. W. *Coord. Chem. Rev.* **1997**, *166*, 181−223.

(7) Zamble, D. B.; Lippard, S. J. In *Cisplatin: Chemistry and Biochemistry of a Leading Anticancer Drug*; Lippert, B., Ed.; Wiley-VCH: Weinheim, 1999; pp 73−110.

(8) Fouts, C. S.; Marzilli, L. G.; Byrd, R. A.; Summers, M. F.; Zon, G.; Shinozuka, K. *Inorg. Chem.* **1988**, *27*, 366−376.

(9) Berners-Price, S. J.; Frenkiel, T. A.; Ranford, J. D.; Sadler, P. J. *J. Chem. Soc., Dalton Trans.* **1992**, 2137−2139.

(10) Sherman, S. E.; Gibson, D.; Wang, A. H.-J.; Lippard, S. J. *Science (Washington, D.C.)* **1985**, *230*, 412−417.

(11) Mukundan, S., Jr.; Xu, Y.; Zon, G.; Marzilli, L. G. *J. Am. Chem. Soc.* **1991**, *113*, 3021−3027.

(12) Caradonna, J. P.; Lippard, S. J. *Inorg. Chem.* **1988**, *27*, 1454−1466.

(13) Neumann, J.-M.; Tran-Dinh, S.; Girault, J.-P.; Chottard, J.-C.; Huynh-Dinh, T. *Eur. J. Biochem.* **1984**, *141*, 465−472.

(14) Kline, T. P.; Marzilli, L. G.; Live, D.; Zon, G. *J. Am. Chem. Soc.* **1989**, *111*, 7057−7068.

(15) den Hartog, J. H. J.; Altona, C.; van der Marel, G. A.; Reedijk, J. *Eur. J. Biochem.* **1985**, *147*, 371−379.

(16) Admiraal, G. A.; van der Veer, J.; de Graff, R. A.; den Hartog, J. H. J.; Reedijk, J. *J. Am. Chem. Soc.* **1987**, *109*, 592−594.

10.1021/ja9916409 CCC: $18.00 
Published on Web 09/18/1999

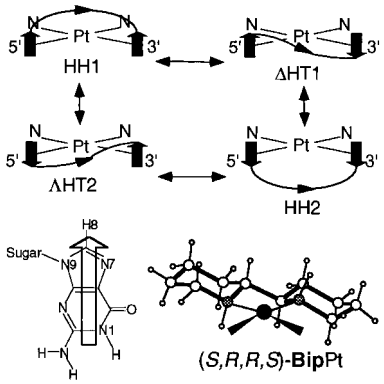


**Figure 1.** G orientations possible in (*S*,*R*,*R*,*S*)-**Bip**Pt(d(GpG)) adducts. In the scheme, the G coordination sites are forward, and the **Bip** ligand is to the rear and shown at the bottom, right. The large arrows within the adducts represent the G bases (as shown at bottom, left), and the small arrows indicate the direction of the propagation of the phosphodiester linkage.

the authors conclude that the HH1 conformer predominates.[11,14,17−20] The G bases in the less common interstrand DNA cross-link are in a head-to-tail (HT) arrangement (Figure 1).[21,22] No definitive identification has been made of HT conformers in N7−Pt−N7 intrastrand d(GpG) cross-links; we report such a species as an abundant conformer for the first time.

An extensive effort involving the testing of more than 3000 compounds has been made to identify carrier ligands giving analogues with activity superior to that of cisplatin; however, no clearly superior carrier ligand has been found.[6,23] The leading experimentally supported biological hypothesis explaining cisplatin anticancer activity involves specific recognition of kinked DNA adducts by proteins with an HMG domain.[7,24−30] Tight binding to the HMG-containing protein is required for such recognition, which by inhibiting repair leads to cell death. The most favorable protein−DNA contacts are likely to involve a specific DNA conformation, and, indeed, even variations in the flanking sequence influence protein binding.[28] However, carrier ligands that favor an alternative base orientation could form DNA adducts which bind more weakly and are thus repaired, and repair diminishes activity. Our work demonstrates that some carrier ligands do favor alternative forms; thus, it is important to identify the nature of these alternative forms and to understand

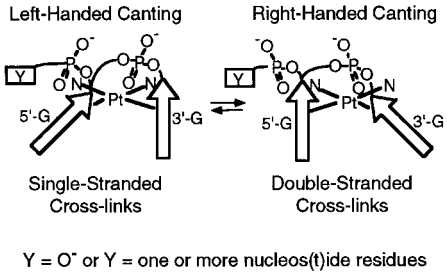


**Figure 2.** Illustration of the HH1 canting variants, HH1 L (left) and HH1 R (right), generally accepted for *cis*-Pt(NH$_3$)$_2$(d(GpG)) adducts.

the features of the carrier ligand that promote populations of atypical structures. Such non-HH1 forms may be the reason that superior carrier ligands are difficult to identify by random screening. However, the fluxional nature of DNA adducts (see below) makes the presence of these alternative base arrangements difficult to detect. Therefore, these forms have not been considered in drug design or in hypotheses advanced to explain activity.

In addition to being present in the rare difunctional adducts of DNA in which nonadjacent bases are cross-linked, HT forms prevail in simple *cis*-PtA$_2$**G**$_2$ complexes (the boldface **G** indicating a guanine derivative not linked to other guanines by a phosphodiester linkage).[31−39] While the HH base orientation is intrinsically achiral, the HT arrangement leads to two chiralities, ΔHT and ΛHT (Figure 1). Relative to HH forms, HT forms are stabilized by favorable dipole or van der Waals interactions between the two guanine bases. It has generally been thought that the sugar−phosphate backbone linking adjacent G bases has the primary effect of stabilizing the HH1 form and that only this form is sterically feasible. The common HH1 conformer has two recognized variants differing in base canting direction (left-handed, L, with the 5′-G base canted toward the 3′-G, and right-handed, R, with the 3′-G base canted toward the 5′-G, Figure 2). The L and R variants are believed to dominate in typical single- and double-stranded HH d(GpG) adducts, respectively.[11,14,15,19,40−42] Thus, the literature suggests an apparent marked dichotomy between the base arrangements in linked (with no HT form known)[43] and unlinked (with the HH form rare, existing as minor species when found)[43] adducts.

The evidence underlying this proposed dichotomy has been interpreted assuming that the processes interconverting the HT

(17) Berners-Price, S. J.; Corazza, A.; Guo, Z.; Barnham, K. J.; Sadler, P. J.; Ohyama, Y.; Leng, M.; Locker, D. *Eur. J. Biochem.* **1997**, *243*, 782−791.
(18) Berners-Price, S. J.; Barnham, K. J.; Frey, U.; Sadler, P. J. *Chem. Eur. J.* **1996**, *2*, 1283−1291.
(19) den Hartog, J. H. J.; Altona, C.; Chottard, J.-C.; Girault, J.-P.; Lallemand, J.-Y.; de Leeuw, F. A. A. M.; Marcelis, A. T. M.; Reedijk, J. *Nucleic Acids Res.* **1982**, *10*, 4715−4730.
(20) van Boom, S. S. G. E.; Yang, D.; Reedijk, J.; van der Marel, G. A.; Wang, A. H.-J. *J. Biomol. Struct. Dyn.* **1996**, *13*, 989−998.
(21) Huang, H.; Zhu, L.; Reid, B. R.; Drobney, G. F.; Hopkins, P. B. *Science (Washington, D.C.)* **1995**, *270*, 1842−1845.
(22) Paquet, F.; Pérez, C.; Leng, M.; Lancelot, G.; Malinge, J.-M. *J. Biomol. Struct. Dyn.* **1996**, *14*, 67−77.
(23) Sandman, K. E.; Lippard, S. J. In *Cisplatin: Chemistry and Biochemistry of a Leading Anticancer Drug*; Lippert, B., Ed.; Wiley-VCH: Weinheim, 1999; pp 523−536.
(24) Ohndorf, U.-M.; Rould, M. A.; He, Q.; Pabo, C.; Lippard, S. J. *Nature* **1999**, *399*, 708−712.
(25) Crul, M.; Schellens, J. H. M.; Beijnen, J. H.; Maliepaard, M. *Cancer Treatment Rev.* **1997**, *23*, 341−366.
(26) Naegeli, H. *FASEB J.* **1995**, *9*, 1043−1050.
(27) Ohndorf, U.-M.; Whitehead, J. P.; Raju, N.; Lippard, S. J. *Biochemistry* **1997**, *36*, 14807−14815.
(28) Dunham, S. U.; Lippard, S. J. *Biochemistry* **1997**, *36*, 11428−11436.
(29) Trimmer, E. E.; Zamble, D. B.; Lippard, S. J.; Essigmann, J. M. *Biochemistry* **1998**, *37*, 352−362.
(30) Patrick, S. M.; Turchi, J. J. *Biochemistry* **1998**, *37*, 8808−8815.
(31) Lippert, B. *Prog. Inorg. Chem.* **1989**, *37*, 1−97.
(32) Miller, S. K.; Marzilli, L. G. *Inorg. Chem.* **1985**, *24*, 2421−2425.
(33) Reily, M. D.; Marzilli, L. G. *J. Am. Chem. Soc.* **1986**, *108*, 6785−6793.
(34) Xu, Y.; Natile, G.; Intini, F. P.; Marzilli, L. G. *J. Am. Chem. Soc.* **1990**, *112*, 8177−8179.
(35) Williams, K. M.; Cerasino, L.; Intini, F. P.; Natile, G.; Marzilli, L. G. *Inorg. Chem.* **1998**, *37*, 5260−5268.
(36) Marzilli, L. G.; Intini, F. P.; Kiser, D.; Wong, H. C.; Ano, S. O.; Marzilli, P. A.; Natile, G. *Inorg. Chem.* **1998**, *37*, 6898−6905.
(37) Kiser, D.; Intini, F. P.; Xu, Y.; Natile, G.; Marzilli, L. G. *Inorg. Chem.* **1994**, *33*, 4149−4158.
(38) Wong, H. C.; Coogan, R.; Intini, F. P.; Natile, G.; Marzilli, L. G. *Inorg. Chem.* **1999**, *38*, 777−787.
(39) Wong, H. C.; Intini, F. P.; Natile, G.; Marzilli, L. G. *Inorg. Chem.* **1998**, *38*, 1006−1014.
(40) den Hartog, J. H. J.; Altona, C.; van Boom, J. H.; van der Marel, G. A.; Haasnoot, C. A. G.; Reedijk, J. *J. Biomol. Struct. Dyn.* **1985**, *2*, 1137−1155.
(41) Herman, F.; Kozelka, J.; Stoven, V.; Guittet, E.; Girault, J.-P.; Huynh-Dinh, T.; Igolen, J.; Lallemand, J.-Y.; Chottard, J.-C. *Eur. J. Biochem.* **1990**, *194*, 119−133.
(42) Yang, D.; van Boom, S. S. G. E.; Reedijk, J.; van Boom, J. H.; Wang, A. H.-J. *Biochemistry* **1995**, *34*, 12912−12920.
(43) Ano, S. O.; Kuklenyik, Z.; Marzilli, L. G. In *Cisplatin: Chemistry and Biochemistry of a Leading Anticancer Drug*; Lippert, B., Ed.; Wiley-VCH: Weinheim, 1999; pp 247−291.

and HH1 forms of linked adducts are slow; it is implicit that any HT form present would be detected by NMR methods or perhaps even by chromatography. The failure to detect an HT form led to the belief that this form did not exist. We have raised counter-arguments to this slow dynamic motion assumption.[43−45] In particular, we note that, since the low symmetry of a DNA chain makes each atom unique, NMR methods cannot easily distinguish the presence of one conformer in a relatively fixed state (the widely believed situation) from the presence of a mixture of conformers in rapid dynamic motion. Rapidly interchanging conformers also would escape detection by chromatography. Thus, the evidence relevant to the linked adducts is suspect. However, simple *cis*-$PtA_2\mathbf{G}_2$ models have symmetrical conformers with more revealing NMR spectra. The NMR data demonstrate that these are highly fluxional, interconverting rapidly between forms in which the bases rotate through ∼180°.[44]

In adducts with the *cis*-$Pt(NH_3)_2$ moiety, the attachment of each $NH_3$ ligand to Pt by a single bond allows each ligand to adopt numerous orientations that permit the NH groups of each ligand to form hydrogen bonds to the nucleic acid target. The orientation of each $NH_3$ is independent of the orientation of the other $NH_3$. Also, this independence and the small size of the NH groups diminish steric interactions with the target. As a consequence, the barriers between the conformers are probably shallow, making *cis*-$Pt(NH_3)_2$ adducts especially fluxional. Furthermore, the guanine bases are likely to wag back and forth with the relative canting of the bases with respect to each other fluctuating with time (Figure 2). Thus, it is not clear whether the propensity of the $(NH_3)_2$ carrier ligand to favor the HH1 conformer is similar to or different from those of other carrier ligands.

**Retro Models.** The cisplatin species is one of the simplest possible molecules. It is the simplicity of the molecule and the dynamic nature of the adducts which has impeded the elucidation of its properties. In fact, since the features are very simple, we are finding that many previous interpretations of these properties are not correct. In contrast to the simplification involved in most modeling of biological/medical systems, we are using a "retro-modeling" approach, wherein we introduce complexity into the carrier ligand both to make the spectral properties more informative and to diminish the dynamic motion.

The specific key feature in our retro-modeling efforts to detect and to characterize new cross-link forms is our use of specially designed ligands that are able to decrease fluxional motions by virtue of possessing rigid bulk along the coordination plane. Since these ligands lack significant bulk above and below the coordination plane, many conformations are possible for nucleic acid adducts. Furthermore, we have incorporated secondary amines near chiral carbons; these carbons restrict the amine configuration to a particular chirality.[34−39,45,46] This design strategy has evolved to our recent use of 2,2′-bipiperidine (**Bip**);[45,46] the coordinated **Bip** ligand has two energetically favored $C_2$-symmetrical geometries, with *S*,*R*,*R*,*S* or *R*,*S*,*S*,*R* configurations at the asymmetric N, C, C, and N chelate ring atoms. The *S*,*R*,*R*,*S* configuration is shown in Figure 1. Since ligands such as **Bip** were found to control the chirality of the HT conformers,[36] we call them chirality-controlling chelate (**CCC**) ligands. (*Note that we denote diamine carrier ligands in boldface type.*)

**New Forms and Properties Revealed by CCC Complexes.** The outstanding ability of the **Bip** ligand to reduce fluxional motion, validating our design, was first established in studies of the distribution of the initially formed **Bip**Pt(5′-GMP)$_2$ rotamers.[43,46,47] More recently, the special features of the **Bip** ligand allowed us to discover a novel (*R*,*S*,*S*,*R*)-**Bip**Pt(d(GpG)) cross-link that was formed in abundance comparable to that of the accepted HH1 conformer in the reaction of d(GpG) with [(*R*,*S*,*S*,*R*)-**Bip**Pt$(H_2O)_2]^{2+}$.[45] This second major adduct was also an HH conformer (HH2, Figure 1); HH2 differs from the widely recognized HH1 form primarily in the propagation direction of the sugar−phosphodiester−sugar linkage. Otherwise, this backbone linkage has a similar structure in both HH conformers of the (*R*,*S*,*S*,*R*)-**Bip**Pt(d(GpG)) cross-link. Even the "normal" HH1 conformer was unusual; this conformer favors the R variant, whereas all previously studied and well-characterized HH1 conformers in single strands appear to be the L variant in solution.

The study of (*R*,*S*,*S*,*R*)-**Bip**Pt(d(GpG)) provided the first definitive evidence for a second HH conformer and the first evidence for this second backbone propagation in a cross-link, a finding that doubled the number of HH conformers to be considered in evaluating intrastrand adducts. If we define the direction of backbone propagation with respect to the HH forms, then the ΔHT form can be designated as ΔHT1 and the ΛHT form as ΛHT2 (Figure 1). The numbers refer to normal (1) and the new (2) propagation directions. These four designations (HH1, HH2, ΔHT1, and ΛHT2) are the principal way in which we shall denote conformers. All four conformers have numerous variants differing in base canting or in torsion angles involving the glycosyl bond, the phosphodiester group, and the deoxyribose ring. For simplicity, we will usually designate only the *syn*/*anti* glycosyl torsion angle for the 5′-G and the 3′-G residues. Thus, there are four possible combinations for each form, giving a total of 16 combinations.

All examples of the 16 combinations are not likely to be found. Usually there are only one or two forms with >30% abundance. However, other forms may be intermediates in the dynamic pathways by which the more stable HT and HH conformers interconvert via rotations about the Pt−N7 and d(GpG) single bonds. Such species and such rotational motions may be critical features in the pathway for the formation of cross-link lesions when *cis*-type Pt drugs react with DNA.[32,33,48−50]

We report here our findings on the products of the reaction of d(GpG) with [(*S*,*R*,*R*,*S*)-**Bip**Pt$(H_2O)_2]^{2+}$, the enantiomer of the previously studied [(*R*,*S*,*S*,*R*)-**Bip**Pt$(H_2O)_2]^{2+}$.[45] This reaction yielded two major products, the normal HH1 form and a new form. Unlike the novel (*R*,*S*,*S*,*R*)-**Bip**Pt(d(GpG)) HH2 conformer, however, the novel (*S*,*R*,*R*,*S*)-**Bip**Pt(d(GpG)) conformer has a distinctly different and new H8 $^1$H NMR chemical shift separation and an unusual upfield $^{31}$P NMR signal. $^1$H NMR data indicate that the new (*S*,*R*,*R*,*S*)-**Bip**Pt(d(GpG)) HT conformer has a *syn* G; this is the first time that such a species has been observed as a major conformer in an N7−Pt−N7 d(GpG) cross-link. Of additional importance, the spectral properties we

(44) Isab, A.; Marzilli, L. G. *Inorg. Chem.* **1998**, *37*, 6558−6559.
(45) Ano, S. O.; Intini, F. P.; Natile, G.; Marzilli, L. G. *J. Am. Chem. Soc.* **1998**, *120*, 12017−12022.
(46) Ano, S. O.; Intini, F. P.; Natile, G.; Marzilli, L. G. *J. Am. Chem. Soc.* **1997**, *119*, 8570−8571.
(47) Ano, S. O.; Intini, F. P.; Natile, G.; Marzilli, L. G. *Inorg. Chem.* **1999**, *38*, 2989−2999.
(48) Dijt, F. J.; Canters, G. W.; den Hartog, J. H. J.; Marcelis, A. T. M.; Reedijk, J. *J. Am. Chem. Soc.* **1984**, *106*, 3644−3647.
(49) Marcelis, A. T. M.; van Kralingen, C. G.; Reedijk, J. *J. Inorg. Biochem.* **1980**, *13*, 213−222.
(50) Marcelis, A. T. M.; Korte, H.-J.; Krebs, B.; Reedijk, J. *Inorg. Chem.* **1982**, *21*, 4059−4063.

have observed require a new interpretation of the solution structure of *cis*-Pt($NH_3$)$_2$(d(GpG)) and of the factors influencing the spectral features of this simplest model and of larger oligonucleotide adducts containing the *cis*-Pt($NH_3$)$_2$(d(GpG)) cross-link.

## Experimental Section

**Materials.** Deoxyguanyl(3′-5′)deoxyguanosine (d(GpG)) from Sigma was used as received. The purity of the free bipiperidine ligand isomers (prepared by hydrogenation of bipyridine)[51] was checked by HPLC using a *RR*-DACH DNB column.

The general preparation of the **Bip**$PtCl_2$ and **Bip**Pt($NO_3$)$_2$ complexes has been described elsewhere.[45] Here, the *R,R* isomer of **Bip** was used. Anal. Calcd for (*S,R,R,S*)-**Bip**$PtCl_2$ ($C_{10}H_{20}Cl_2N_2Pt$): C, 27.7; H, 4.6; N, 6.4. Found: C, 27.6; H, 4.7; N, 6.3. Anal. Calcd for (*S,R,R,S*)-**Bip**Pt($NO_3$)$_2$ ($C_{10}H_{20}N_4O_6Pt$): C, 24.6; H, 4.1; N, 11.5. Found: C, 24.8; H, 4.1; N, 11.5.

**Methods.** In a typical in situ preparation, d(GpG) (1 equiv) was treated with (*S,R,R,S*)-**Bip**Pt($NO_3$)$_2$ (1 equiv, ∼0.8 mM) in $D_2O$ (2−4 mL) at pH 3.5 and 0 °C; concentrated (∼3 mM) or pH 7 conditions were sometimes employed. Reactions were monitored by $^1$H NMR spectroscopy until no free d(GpG) signal or no change in H8 signal intensity was observed. Samples were eventually lyophilized and redissolved in 99.96% $D_2O$ for 2D NMR experiments.

1D NMR spectra were obtained on a GE GN600 Omega spectrometer and referenced to the residual HOD peak ($^1$H)[52] or trimethyl phosphate ($^{31}$P). The saturation transfer experiments used a 16K block size and a presaturation pulse sequence with a 500-ms delay. For homonuclear 2D data, a 256 (or 512) × 2048 matrix was typically collected at 5 °C with a 6250-Hz spectral width and processed using Felix 2.3 (Molecular Simulations, Inc.). Each acquisition included a 2-s presaturation pulse and a 10-ms delay. Data were apodized using an exponential multiplication with a line broadening of 1−2 Hz in $t_2$ and a 90° phase-shifted squared sine bell along 256 points in $t_1$. The evolution dimension was zero-filled to 2K prior to Fourier transformation.

Phase-sensitive nuclear Overhauser enhancement spectroscopy (NOESY) data[53−55] were collected with 128 scans per $t_1$ increment, 300 ms mixing time. A 2D double-quantum filtered correlation spectroscopy (DQF COSY)[56] experiment was performed using 256 scans per $t_1$ increment. In processing, the first point in $t_1$ was multiplied by 0.5.

Relevant parameters for the 2D $^1$H−$^{31}$P reverse chemical shift correlation (RCSC) experiment[57] include the following: 5 °C, 160 scans per $t_1$ increment, a 2200-Hz spectral window (includes the H3′, H4′, and H5′/5″ regions) in the $^1$H dimension, a 1000-Hz spectral window in the $^{31}$P dimension, and a 100-ms relaxation delay. The data were processed using a 90° phase-shifted squared sine bell along $t_2$ and $t_1$ (1024 and 128 points, respectively).

The HPLC analysis was performed with a Waters system equipped with a U6-K universal injector, a model 626 solvent delivery system, UV/vis detector models 481 and 486, and a Millennium 2010 workstation. Operating conditions were as follow: column, LiChrosorb RP18 5 $\mu$m, 250 × 4 mm i.d.; column temperature, 30 °C; mobile phase, water (0.02 M ammonium acetate buffer, pH 5.5) and aqueous methanol (2:1 v/v, 0.02 M ammonium acetate buffer, pH 5.5), 60:40 (v/v); flow rate, 0.70 mL/min; detector set at 254 nm; operating pressure, 2300 psi. The lyophilized sample, dissolved in water, gave a chromatogram showing three main peaks, assigned by relative abundance, with retention times of ∼15 (HH), 28 (HT), and 32.5 min (unknown) with a relative abundance, HH > HT > unknown. The three eluted fractions were concentrated to a small volume (0.5 mL) and stored in the refrigerator (−20 °C). The unknown species eluting at 32.5 min is a minor product that was observed only after times longer than those required for equilibration of the HH and HT forms.

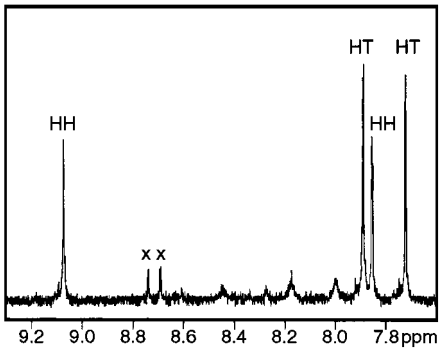


**Figure 3.** H8 $^1$H NMR signals of (*S,R,R,S*)-**Bip**Pt(d(GpG)) at pH ∼3.5, 20 °C (× marks signals of a third d(GpG) adduct mentioned in the text and observed reproducibly. The very small broad minor signals at ∼8.45 and ∼8.25 ppm were not usually observed. The small broad minor signals at ∼8.2 and ∼8.0 ppm arise from a slight excess of d(GpG)).

For kinetic studies, the HPLC fraction of the pure HH or HT isomer and ammonium acetate buffer (∼0.4 M) was brought to the desired pH (pH 3.4 by addition of nitric acid (0.5 M) and pH 7.0 by addition of ammonium hydroxide (0.9 M)) and kept at 40 °C. An aliquot was injected, at ∼1-h intervals, into the chromatograph, and the percentage of each peak was measured by integration of the corresponding peak area.

Molecular mechanics and dynamics (MMD) calculations were performed using the procedures described previously.[45] The force field used for modeling was recently developed in this laboratory.[58]

## Results

**Product Formation and Redistribution.** Two major (*S,R,R,S*)-**Bip**Pt(d(GpG)) products in the reaction mixture of d(GpG) with [(*S,R,R,S*)-**Bip**Pt($H_2O$)$_2$]$^{2+}$ were indicated by two pairs of large H8 NMR signals (Figure 3; NMR spectral changes ceased after ∼8 h under these conditions, pH ∼3.5, 0 °C). The signals did not shift from pH 3.5 to 1.3, indicating N7 coordination by both G residues in both products.[59] Initially we refer to the two main products only by the relative HH or HT base orientations determined by 2D NMR data (see below). Also below, we show that the two products interconvert very slowly under normal formation reaction conditions (0.8 mM, pH 3.5, 0 °C). The final HT:HH H8 signal ratio of 60:40 (at 0−5 °C) after the NMR spectral changes are complete is a kinetically (not thermodynamically) determined ratio.

The present study focuses on the properties and conformation of the two major (*S,R,R,S*)-**Bip**Pt(d(GpG)) conformers that exist at equilibrium, with the primary emphasis on the unprecedented ΔHT1 conformer. The complicated process of cross-link formation from reactants itself deserves separate study in the future, and it will be mentioned here only in the context of understanding the nature of the two major adducts. A third kinetic product, characterized by a pair of downfield H8 signals, is initially (∼20 min into the reaction) present at about the same level as the two main products, but it soon becomes a minor species and

(51) Sato, M.; Sato, Y.; Yano, S.; Yoshikawa, S.; Toriumi, K.; Itoh, H.; Itoh, T. *Inorg. Chem.* **1982**, *21*, 2360−2364.
(52) Hoffman, R. E.; Davies, D. B. *Magn. Reson. Chem.* **1988**, *26*, 523−525.
(53) Jeener, J.; Meier, B. H.; Bachmann, P.; Ernst, R. R. *J. Chem. Phys.* **1979**, *71*, 4546−4553.
(54) Kumar, A.; Ernst, R. R.; Wüthrich, K. *Biochem. Biophys. Res. Commun.* **1980**, *95*, 1−6.
(55) States, D. J.; Haberkorn, R. A.; Ruben, D. J. *J. Magn. Reson.* **1982**, *48*, 286−292.
(56) Bodenhausen, G. *Prog. NMR Spectrosc.* **1981**, *14*, 137−173.
(57) Sklenár, V.; Miyashiro, H.; Zon, G.; Miles, H. T.; Bax, A. *FEBS Lett.* **1986**, *208*, 94−98.
(58) Yao, S.; Plastaras, J. P.; Marzilli, L. G. *Inorg. Chem.* **1994**, *33*, 6061−6077.
(59) Girault, J.-P.; Chottard, G.; Lallemand, J.-Y.; Chottard, J.-C. *Biochemistry* **1982**, *21*, 1352−1356.

appears to redistribute into both the HH and HT products. We believe that the greater amount of the HT form over the HH form observed during all but the earliest stage of the formation reaction is largely due to the preferential formation of the HT form by this third product. When the spectral changes are complete (typically several hours for various reaction conditions), this third product is present in too small an amount to characterize. Thus, it is kinetically favored but thermodynamically unfavored. Furthermore, the H8 signals of this third adduct did not shift when the pH was lowered to 1.3, indicating N7 coordination of both G's.

All evidence clearly points to the two main products being monomers, as found previously for (*R,S,S,R*)-**Bip**Pt(d(GpG)).[45] The MALDI mass spectrum of an NMR sample has a mass ion at *m*/*z* 962, close to the value of 959 expected for the (*S,R,R,S*)-**Bip**Pt(d(GpG)) monomer. Comparison of the 1:1 reaction at pH 3.5, 0 °C, monitored by $^1$H NMR spectroscopy, carried out under dilute (0.8 mM) and concentrated (∼3 mM) conditions gave the same main products and product distribution after ∼8 h, another indication that the products are monomers. Furthermore, when *rac*-**Bip**Pt$(NO_3)_2$ was treated with d(GpG) using dilute conditions and 0 °C, the only product H8 signals observed after 150 min corresponded to those of the products of reactions with the separate [**Bip**Pt$(H_2O)_2]^{2+}$ enantiomers (Supporting Information).[45] This observation rules out the possibility that the main products are 2:2 adducts since new H8 signals attributable to a mixed (*S,R,R,S*)-**Bip**Pt:(*R,S,S,R*)-**Bip**Pt:$(d(GpG))_2$ species would have been observed. Also, the reaction of [(*S,R,R,S*)-**Bip**Pt$(H_2O)_2]^{2+}$ with d(GpG) at pH 7 formed primarily the same products as the reaction at pH 3.5, with the HT conformer more abundant (HT:HH = 55:45), indicating that the chirality of the N center in the **Bip**Pt moiety is preserved and that pH has little influence on product formation.

Saturation transfer experiments showed that no transfer of magnetization occurred between the H8 signals of the (*S,R,R,S*)-**Bip**Pt(d(GpG)) conformers at 55 °C, indicating slow interconversion of the two conformers. However, at ∼55 °C, the relative intensities of the H8 signals changed, and the HH product became the major conformer (60−65% after 2 h). This ratio did not change further up to 24 h at 55 °C. Equilibration at 40 °C of the HH and HT forms, separated by HPLC, gave pH-independent equilibration rate constants ($3.65 \times 10^{-5}$ s$^{-1}$ at pH 3.4 and $3.46 \times 10^{-5}$ s$^{-1}$ at pH 7, Supporting Information). From an average of these rate constants ($\sim 3.5 \times 10^{-5}$ s$^{-1}$), a half-life of 330 min was calculated for the redistribution of pure HH (or HT) form to an equilibrium mixture at 40 °C. The HPLC data demonstrate that the **Bip** configuration, as expected, is the same in the HH and HT forms since a change in configuration would require base-catalyzed inversion at one NH, and the rate would be faster at pH 7.

**Base Orientations.** In the foregoing section, we established that the (*S,R,R,S*)-**Bip**Pt(d(GpG)) products are isomers. In this section, we present the key features that show that the bases in the HT form, indeed, have the HT arrangement unprecedented for an N7−Pt−N7 d(GpG) cross-linked adduct.

An H8−H8 NOE cross-peak has been observed for all known N7−Pt−N7 d(GpG) cross-links so studied. In the (*S,R,R,S*)-**Bip**Pt(d(GpG)) NOESY spectrum (Figure 4), the presence of this cross-peak for the HH form is the primary evidence indicating that this product has the common HH base orientation, while the absence of this cross-peak for the HT product strongly suggests the HT N7−Pt−N7 d(GpG) cross-link. Furthermore, all known HH forms have at least one relatively downfield (>∼8.5 ppm) H8 signal.[2,8,11,15,19] Indeed, the HH form of the

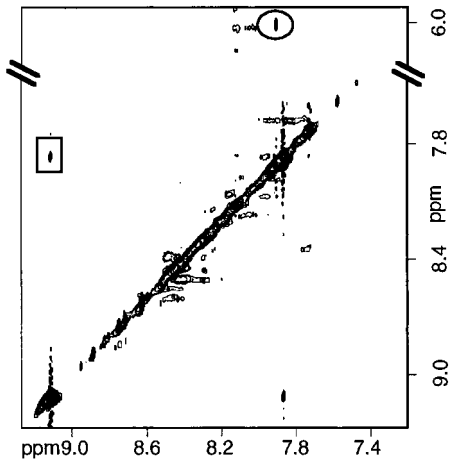


**Figure 4.** H8−H8 and H8−H1′ regions of the 2D NOESY spectrum of (*S,R,R,S*)-**Bip**Pt(d(GpG)) at pH 3.5, 5 °C. The H8−H8 NOE cross-peak of the HH conformer and the 3′-G H8−H1′ NOE cross-peak of the HT conformer are boxed and circled, respectively.

(*S,R,R,S*)-**Bip**Pt(d(GpG)) adduct has one downfield (∼9.1 ppm) H8 signal, supporting the presence of the HH base orientation in this form. However, *both* H8 signals of the HT form were *upfield*. This unusual finding indicates a unique N7−Pt−N7 d(GpG) cross-link conformation with both H8's in a highly shielding environment; this H8 shielding (caused by the ring current of the cis G) counteracts the H8 deshielding effect of N7 platination.

Other aspects of the experimental data suggest that the HT form is very unusual. First, all clearly defined HH N7−Pt−N7 cross-links have a $^{31}$P NMR signal downfield of the typical −4.2 ppm value of unstrained phosphodiester groups;[60] see, for example, the HH conformers of (*R,S,S,R*)-**Bip**Pt(d(GpG)) (Table 1).[45] The upfield $^{31}$P shift of the HT form at −4.6 ppm (Table 1) is thus evidence that the HT form is not an HH form. Second, the 5′-G H3′ and 3′-G H2′ signals of the HT form have unusual chemical shifts (Table 1). Third, the 3′-G sugar proton coupling pattern indicates that this residue has a sugar with a high percentage of N character in the HT form, whereas N7−Pt−N7 d(GpG) HH intrastrand cross-links have a 3′-G sugar pucker with little N character. Finally, we note that the H8 signal separation in the HT conformer (0.18 ppm) is unusually small, an uncommon feature for HH forms.[61,62]

**NMR and Conformational Assignments.** DQF COSY and NOESY data were used to assign $^1$H NMR signals (Table 1) and determine the HH and HT conformations. The specific details are provided in Supporting Information. At 25 °C, $^{31}$P NMR signals at −2.8 and −4.6 ppm were assigned to the HH and HT conformers, respectively, on the basis of signal integration. Here we mention only the presence of a strong 3′-G H1′−H8 NOE cross-peak (Figure 4) and the absence of any 3′-G H8−H2′/2″ NOE cross-peaks, results indicating that the 3′-G is in a *syn* conformation. This conformation is defined by the $\chi$ (C4−N9−C1′−O4′) angle. The values from the modeling studies (see below) for $\chi$ and the pseudorotation phase angle, *P*, are given in Table 2, and the definitions are described in depth in the Supporting Information.

**Sugar Pucker.** All HH N7−Pt−N7 GpG intrastrand cross-links have a 5′-G N sugar.[10,45,59,63] Normally, one indication of

(60) Gorenstein, D. G. In *Phosphorus-31 NMR. Principles and Applications*; Gorenstein, D. G., Ed.; Academic Press: Orlando, FL, 1984; pp 7−36.
(61) Hambley, T. W.; Ling, E. C. H.; Messerle, B. A. *Inorg. Chem.* **1996**, *35*, 4663−4668.
(62) Dunham, S. U.; Lippard, S. J. *J. Am. Chem. Soc.* **1995**, *117*, 10702−10712.

**Table 1.** $^1$H and $^{31}$P NMR Assignments for (*S,R,R,S*)-**Bip**Pt(d(GpG)) from 2D NMR Data[a] and Relevant Data from the Literature

| d(GpG) species | G | H8 | H1′ | $J_{H1'-H2'}/J_{H1'-H2''}$[b] | H2′ | H2″ | H3′ | H4′ | $^{31}$P |
|---|---|---|---|---|---|---|---|---|---|
| (*S,R,R,S*)-**Bip**Pt(d(GpG)) HH1 | 5′ | 7.88 | 5.92 | 0.0/7.1 (d) | 2.28 | 2.71 | 4.99 | 4.01 | −2.8 |
| | 3′ | 9.11 | 6.27 | 9.6/4.2 (dd) | 2.77 | 2.48 | 4.71 | 4.21 | |
| (*S,R,R,S*)-**Bip**Pt(d(GpG)) ΔHT1 | 5′ | 7.77 | 6.17 | 0.0/5.4 (d) | 2.72 | 2.58 | 3.90 | − | −4.6 |
| | 3′ | 7.91 | 6.01 | 3.0/8.0 (dd) | 3.29 | 2.44 | 4.95 | 3.99 | |
| (*R,S,S,R*)-**Bip**Pt(d(GpG)) HH1[c] | 5′ | 8.76 | 6.32 | 0.0/6.8 (d) | 2.48 | 2.73 | 4.82 | 4.13 | −3.2 |
| | 3′ | 8.22 | 6.23 | 9.5/4.9 (dd) | 2.32[d] | 2.37[d] | 4.54 | 4.16 | |
| (*R,S,S,R*)-**Bip**Pt(d(GpG)) HH2[c] | 5′ | 8.30 | 6.17 | 0.0/7.4 (d) | 2.94 | 2.76 | 4.49 | 3.97 | −2.6 |
| | 3′ | 8.70 | 6.15 | 8.3/5.0 (dd) | 2.35 | 2.78 | 4.66 | 4.46 | |
| *cis*-Pt(NH$_3$)$_2$(d(GpG))[e] | 5′ | 8.26 | 6.18 | 0.6/7.3 | 2.62 | 2.73 | 4.62 | 4.07 | −3.4 |
| | 3′ | 8.57 | 6.22 | 8.1/6.0 | 2.71 | 2.56 | 4.72 | 4.23 | |
| d(GpG) | 5′ | 7.75[f] | *g* | 8.2/6.7 (dd)[g] | | | | | |
| | 3′ | 8.00[f] | *g* | 9.2/5.6 (dd)[g] | | | | | |

[a] All shifts in ppm; data for 5 °C, pH 3.5 unless stated otherwise. [b] In hertz; at 5−7 °C; digital resolution = 0.4 Hz. [c] Reference 45. [d] H2′/2″ signals could not be distinguished. [e] $^1$H shifts reported at 23 °C, pH 6.5; $^{31}$P shift reported at 27 °C, pH 6.5.[19] [f] Assignments from ref 68. [g] This study; H1′ shift values are 6.1 and 5.97 (not known which is 5′-G or 3′-G), pH 7.2, 7 °C.

**Table 2.** Summary of (*S,R,R,S*)-**Bip**Pt(d(GpG)) Restrained and *cis*-Pt(NH$_3$)$_2$(d(GpG)) Unrestrained MMD Calculations

| model | conformer | *syn* G[a] | energy (kcal/mol) | $\chi$[b](deg) | | *P*[c] (deg) | | 5′-G H8−3′-G H8 (Å) |
|---|---|---|---|---|---|---|---|---|
| | | | | 5′-G | 3′-G | 5′-G | 3′-G | |
| **1** | HH1 | | 10.1 | −90 | −100 | 33 | 132 | 2.80 |
| **2** | HH2 | | 13.6 | −80 | −120 | −13 | 152 | 3.18 |
| **3** | ΔHT1 | 5′-G | 11.3 | −147 | −132 | 28 | 144 | 4.76 |
| **4** | ΔHT1 | 3′-G | 9.5 | −154 | 62 | 53 | 66 | 4.60 |
| **5** | ΛHT2 | 5′-G | 9.9 | 15 | −19 | 15 | 4 | 5.20 |
| *cis*-Pt(NH$_3$)$_2$ | HH1 | | −1.3 | −172 | −136 | 23 | 120 | 2.97 |
| *cis*-Pt(NH$_3$)$_2$ | HH2 | | −4.0 | −90 | 172 | −26 | 158 | 3.17 |
| *cis*-Pt(NH$_3$)$_2$ | ΔHT1 | 3-G′ | −3.2 | −160 | 61 | 55 | 71 | 4.68 |
| *cis*-Pt(NH$_3$)$_2$ | ΛHT2[d] | 5′-G′ | −1.3 | 41 | −8 | 24 | 5 | 4.46 |

[a] *syn* G residue in starting model. [b] $\chi$ = C4−N9−C1′−O4′. [c] *P* = pseudorotation phase angle calculated from the equation, tan *P* = $((\nu_4 + \nu_1) - (\nu_3 + \nu_0))/(2\nu_2(\sin 36° + \sin 72°))$ ($\nu_{0-4}$ are endocyclic sugar torsion angles); $0° \le P \le 36°$ (±18°) corresponds to an N sugar, while $144° \le P \le 190°$ (±18°) indicates an S sugar.[71] [d] The ΛHT2 conformer minimized with two *syn* G residues, regardless of which G residue was *syn* in the starting structure.

this pucker is a strong H8−H3′ NOE cross-peak. For the HT form, no 5′-G H8 sugar (including H3′) NOE cross-peaks were identified, and the *syn* 3′-G residue had no H8−H3′/2′/2″ NOE cross-peaks, as expected since 3′-G H8 is on the opposite side of the sugar from these protons. Thus, we used coupling data to evaluate sugar pucker. The H1′ coupling patterns in the 1D $^1$H NMR spectra (7−45 °C) indicate that the 5′ sugar has predominantly an N pucker (both HH and HT) and that the 3′ sugar has predominantly an S (HH) or N (HT) pucker. Typically, N sugars have only the H1′−H2″ cross-peak in the DQF COSY spectrum.[64] There are only H1′−H2″ DQF COSY cross-peaks and no H1′−H2′ COSY cross-peaks for the 5′-G sugar residues of both HT and HH forms. Thus, the sugar of the 5′-G residue of the HT form, like that of the HH form, favors the N pucker.

The presence of 3′-G H1′−H2′ COSY coupling in the HH form (Supporting Information) and the 1D NMR coupling data (Table 1) are consistent with the HH form having a mainly 3′-G S sugar pucker, normal for a cross-link. However, the HT 3′-G COSY coupling pattern (strong H1′−H2″ and H3′−H2′ couplings and weak H1′−H2′ and H2″−H3′ couplings) indicates a large percentage of N character.[64] It is unprecedented for both sugars of an N7−Pt−N7 cross-link adduct to have an N pucker.

**Molecular Modeling Calculations.** Models potentially consistent with our results were constructed and subjected to MMD calculations using restraints generated from NMR data, leading to five model types (Table 2). Improbable conformers were not modeled. For example, since $^1$H NMR data indicated that the HT form had only one *syn* residue, no *syn*,*syn* starting structures were modeled. In other cases, simple analysis of plastic models shows that a particular conformer was improbable. For example, the ΛHT2 conformation with two *anti* G residues has both G bases canted such that the six-membered ring of the base is unfavorably close to one piperidine ring of the **Bip** ligand. The overall energy of each model structure is the sum of a number of energy terms, some of which may not be weighted correctly in the force field. Thus, all but large energy differences in the modeling results should be interpreted with caution. For comparison, other models were evaluated without the use of restraints; these are discussed below.

Model **1** has HH G's and the normal backbone propagation (HH1) (Figure 5). Model **2** differs from model **1** in the direction of propagation of the backbone (HH2). Both of these models were restrained using the HH form data. The restrained HH2 model was calculated to be less stable than the restrained HH1 model by ∼3 kcal/mol (Table 2), suggesting that the HH form observed here does not have the HH2 conformation.

Of the four (*S,R,R,S*)-**Bip**Pt(d(GpG)) HT models subjected to restrained MMD/energy minimization studies, the ΔHT1 model with a *syn* 3′-G (**4**) had the lowest calculated energy (Table 2). Indeed, this restrained HT model was calculated to be ∼0.5 kcal/mol more stable than the restrained *anti*,*anti* HH1 model (Figure 5).

Model **4** (Figure 5) has a 5′-G O6−NH(**Bip**) hydrogen bond, which cants the 5′-G base toward the 3′-G; the 3′-G base is only very slightly canted (6°) toward the 5′-G base. The 5′-G and 3′-G sugars have puckers close to N (Table 2, Figure 5, and Supporting Information). The $\chi$ torsion angle values for the 5′-G and 3′-G moieties are in the *anti* and *syn* ranges, respectively (Table 2). The out-of-plane bending angle for 3′-G was slightly larger than that for 5′-G (Supporting Information).

(63) Iwamoto, M.; Mukundan, S., Jr.; Marzilli, L. G. *J. Am. Chem. Soc.* **1994**, *116*, 6238−6244.
(64) Widmer, H.; Wüthrich, K. *J. Magn. Reson.* **1987**, *74*, 316−336.

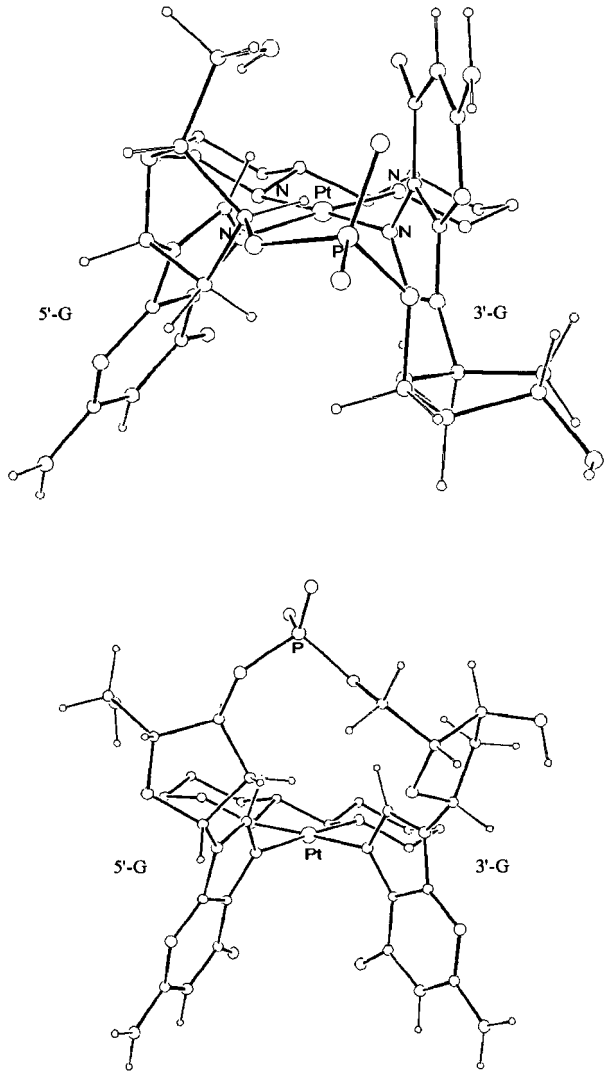


**Figure 5.** Minimum energy models of (*S,R,R,S*)-**Bip**Pt(d(GpG)) from NMR-restrained MMD calculations: *anti,syn* ΔHT1, **4** (top), and *anti,anti* HH1, **1** (bottom).

Similar structural features, including canting, sugar puckers, and H8−H8 distances, were found for the unrestrained ΔHT1 **4** models.

## Discussion

**Coexistence of Multiple Cross-Link Conformers.** Prior to our retro-modeling studies with **Bip**Pt(d(GpG)) adducts, all studies with Pt amine complexes proposing or establishing clearly defined N7−Pt−N7 d(GpG) intrastrand cross-link structures describe HH1 variants with two *anti* G's, except for one case with a *syn* G.[63] The only HH conformation recognized as a possibility for the N7−Pt−N7 d(GpG) intrastrand cross-link was HH1. In both recent and earlier studies, alternative d(GpG) N7−Pt−N7 cross-link forms were subjects of speculation; however, in these speculations the nature of the putative forms was left undefined. Distinct, resolved, multiple forms of simple single-strand GG cross-links were not known.[17,18] There is recent evidence for two forms of an adduct of cisplatin with a double-stranded oligonucleotide.[17,18] Multiple conformers of self-complementary duplexes have also been observed.[20] As mentioned in the Introduction, we recently discovered a second class of conformers, HH2, in our studies on (*R,S,S,R*)-**Bip**Pt-(d(GpG)).[45] The new results presented here for the complex of the enantiomeric **Bip** ligand with the *S,R,R,S* chirality reveal both the existence and the nature of yet a second type of novel conformer, ΔHT1. Both of these novel forms have a stability comparable to that of the well-known HH1 conformer.

We obtained clear evidence for a third N7−Pt−N7 form in this study (cf. Figure 3) and in our previous study of (*R,S,S,R*)-**Bip**Pt(d(GpG)).[45] The third form found in this study can rearrange in minutes at very low temperature, but it is present at too low a level to characterize. Since this form has spectral features different from any in the literature, we have no good basis for speculation as to its conformation. In our study of the (*R,S,S,R*)-**Bip**Pt(d(GpG)) adduct,[45] we noted that the minor form had H8 signals very similar to those of the ΔHT1 form found here for (*S,R,R,S*)-**Bip**Pt(d(GpG)).[45] Thus, even for (*R,S,S,R*)-**Bip**Pt(d(GpG)), an HT form is present, but it is a minor form. The large body of poorly understood spectral features[43] in the literature has led to speculation about dynamic mixtures of multiple conformers of adducts with clinically used drugs. Our experimental results with **Bip**Pt(d(GpG)) adducts and our calculations on *cis*-Pt$(NH_3)_2$(d(GpG)), to be discussed below, also suggest that such dynamic mixtures could exist. Thus, spectral features of adducts with **CCC** ligands such as **Bip** are of clear value for better characterization of conformers that are potentially formed by clinically used drugs. We return to this important topic after we discuss the new results from the present study.

**The HT Conformer.** Both the experimental evidence and the MMD calculations clearly indicate that the HT form is the *anti,syn* ΔHT1 conformer, with a 5′-G N sugar normal for a cross-link but with an unprecedented high percentage of N character for the 3′-G sugar (Table 1). The NMR-restrained *anti,syn* ΔHT1 model **4** has N sugars (or near N sugars) for both the 5′- and 3′-G residues (Table 2), although this MMD model was not derived with either coupling constant or intraresidue H8−H2′/2″/3′ NOE restraints; these types of restraints would influence the sugar pucker in the model. Thus, even without restraints to generate atypical sugar puckers, especially for 3′-G, the ΔHT1 model has sugar puckers in agreement with experimental data. A striking feature emerging from our modeling is that an N sugar was found for the 3′-G residue only for HT models.

In most cross-link adducts, the position of the G base relative to the sugar is difficult to determine because G H8-sugar proton NOE cross-peaks are generally weak. In the restrained *anti,syn* ΔHT1 model **4**, the *syn* 3′-G residue has a short H8−H1′ distance (2.5 Å), consistent with the strong 3′-G H8−H1′ NOE cross-peak. Furthermore, no 3′-G H8−H2′/2″/3′ NOE cross-peaks were observed experimentally, and these distances are all >4.2 Å in this ΔHT1 model. Also in this model, the long 5′-G H8−H1′/H2′/2″/3′ distances (>3.4 Å) are in good agreement with the relatively few NOE cross-peaks observed experimentally.

The relative G base/sugar positioning of the *anti,syn* ΔHT1 model **4** also explains the unusual shifts of the 5′-G H3′ signal at 3.9 ppm and the 3′-G H2′ signal at 3.3 ppm of the HT form (Table 1). Similar shifts have been reported in a hairpin-like structure with a 3′-G *syn* residue.[63] These unusual $^1$H NMR shifts may be diagnostic for identifying 3′-G *syn* residues in intrastrand cross-link d(GpG) adducts. The downfield shift of the H2′ signal in *syn* residues has been noted in a variety of systems.[63,65−68] Of these systems, an upfield H3′ signal was found only in the hairpin-like structure.[63] In the restrained ΔHT1

(65) Kaspárková, J.; Mellish, K. J.; Qu, Y.; Brabec, V.; Farrell, N. *Biochemistry* **1996**, *35*, 16705−16713.
(66) Mao, B.; Cosman, M.; Hingerty, B. E.; Broyde, S.; Patel, D. J. *Biochemistry* **1995**, *34*, 6226−6238.

model, the 5′-G H3′ proton points into the 3′-G base shielding cone, and the 5′-G H3′ to 3′-G six-membered ring distance is 3.2 Å (Figure 5 and Supporting Information); this positioning and distance would shield this H3′, thus accounting for the observed upfield signal. However, the 5′-G H3′ to 3′-G six-membered ring distance is also ~3.2 Å in the other (*S*,*R*,*R*,*S*)-**Bip**Pt(d(GpG)) HT models. The 5′-G H3′ to 3′-G six-membered ring distance is very long in the restrained HH1 and HH2 (*S*,*R*,*R*,*S*)-**Bip**Pt(d(GpG)) models (>6.6 Å). Thus, this upfield 5′-G H3′ shift strongly supports the conclusion that we have, indeed, found an unusual HT form.

The −4.6-ppm $^{31}$P signal of the HT form is only slightly upfield from the −4.2 ppm value normally observed for an unstrained phosphodiester group.[60] We are reluctant to suggest the cause for the upfield shift, since factors influencing such shifts are complicated and the even larger shift changes for HH forms are still not well understood. We note, however, that our $^{31}$P shift is similar to that of another d(GpG) adduct with one *syn* G. This adduct formed by [{*trans*-PtCl($NH_3$)$_2$}$_2${$\mu$-$H_2$N-($CH_2$)$_3$$NH_2$}]$^{2+}$ has different Pt's bound to each G.[68]

**Transient and Minor HT Conformers.** In addition to the abundant form, there are seven other hypothetical HT conformers with various *anti*/*syn* G residue combinations. We briefly note that calculations suggest that two of them, ΛHT2 with two *syn* G residues and ΔHT1 with two *anti* G residues, are the best HT candidates for the observed transient or minor **Bip**Pt(d(GpG)) adducts (Table 2); these might exist in significant abundance with other carrier ligands. In our calculations on the *anti*,*anti* ΔHT1 conformer, we could not use NMR restraints (which would force one G residue to become *syn*). The lowest energy unrestrained model had two G O6−NH(**Bip**) hydrogen bonds, with a calculated energy of 9.6 kcal/mol, a value that is ~3 kcal/mol higher than that of the unrestrained analogue of the *anti*,*syn* ΔHT1 model **4**. The high energies calculated for the other HT models relative to that of the *anti*,*syn* ΔHT1 model are consistent with the presence of only one abundant HT form.

**The HH Form.** The H8−H8 NOE cross-peak (Figure 4) for the (*S*,*R*,*R*,*S*)-**Bip**Pt(d(GpG)) HH form indicates a short (2.88 Å) H8−H8 distance. The H8−H8 distance of the HH1 model (2.8 Å) is in better agreement with the experimental H8−H8 distance than is the distance of the HH2 model (3.18 Å). Our analysis of H8 shifts (see below), as well as other NMR spectral data (Supporting Information) and energetics (Table 2), leaves no doubt that the HH form has the *anti*,*anti* HH1 conformation.

**Carrier Ligand Effects on the ΔHT1 Conformer.** The observation that several N7−Pt−N7 d(GpG) conformers are relatively stable raises new issues relevant to cisplatin adducts. In particular, we examined the role of the carrier ligand in influencing the nature of the conformation of *anti*,*syn* ΔHT1 N7−Pt−N7 cross-links by performing MMD calculations on models of (*R*,*S*,*S*,*R*)-**Bip**Pt(d(GpG)), *cis*-Pt($NH_3$)$_2$(d(GpG)), and (*S*,*R*,*R*,*S*)-**Bip**Pt(d(GpG)). For consistency, the calculations (Supporting Information) were performed without NMR restraints so that structures not observed experimentally could be compared to the *anti*,*syn* ΔHT1 conformer observed here. Calculated energies of the models with different carrier ligands cannot be compared, except for isomers with the same number of terms, including hydrogen bond restraints. The latter were introduced to assess structural features of variants; e.g., (*S*,*R*,*R*,*S*)-**Bip**Pt(d(GpG)) models restrained by one and by two G O6−NH hydrogen bonds were evaluated.

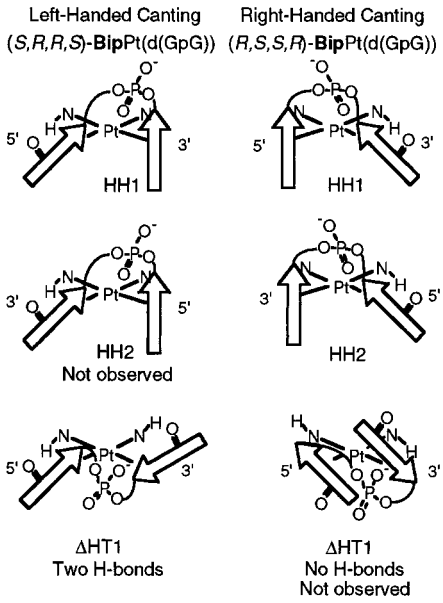


**Figure 6.** Schematic representation of the four variants observed as well as the two variants not observed. The relative position of the O6 of each canted guanine base relative to the *cis* NH of the **Bip** carrier ligand is also illustrated. Note that the (*S*,*R*,*R*,*S*)-**Bip**Pt(d(GpG)) ΔHT1 conformer has the potential to form two G O6−NH hydrogen bonds.

Several structural features are similar for the various ΔHT1 models (Supporting Information). Even without restraints, the *syn* conformation of the 3′-G residue in the starting models of the d(GpG) cross-links was conserved in all the lowest energy structures. All the ΔHT1 models had N sugars for the 5′-G residue. The *anti*,*syn* ΔHT1 model of *cis*-Pt($NH_3$)$_2$(d(GpG)) (Table 2) is structurally very similar to both the restrained and unrestrained *anti*,*syn* ΔHT1 (*S*,*R*,*R*,*S*)-**Bip**Pt(d(GpG)) model **4** (Supporting Information). Thus, the computed structure of this ΔHT1 model of *cis*-Pt($NH_3$)$_2$(d(GpG)) is realistic, and such a conformer should have NMR features similar to those of the (*S*,*R*,*R*,*S*)-**Bip**Pt(d(GpG)) HT form. Furthermore, we find that this conformer has one of the lowest energies of the *cis*-Pt($NH_3$)$_2$(d(GpG)) models (Table 2), suggesting that it could be part of a dynamic mixture of *cis*-Pt($NH_3$)$_2$(d(GpG)) conformers.

Unlike in the *anti*,*syn* ΔHT1 form of (*S*,*R*,*R*,*S*)-**Bip**Pt(d(GpG)) or *cis*-Pt($NH_3$)$_2$(d(GpG)), the G orientations in the *anti*,*syn* ΔHT1 form of (*R*,*S*,*S*,*R*)-**Bip**Pt(d(GpG)) do not allow G O6−NH hydrogen bonds to form (Figure 6). The unrestrained *anti*,*syn* ΔHT1 (*R*,*S*,*S*,*R*)-**Bip**Pt(d(GpG)) model was 1 and 3.3 kcal/mol less stable than the unrestrained HH1 and HH2 (*R*,*S*,*S*,*R*)-**Bip**Pt(d(GpG)) models, respectively. Thus, this *anti*,*syn* ΔHT1 (*R*,*S*,*S*,*R*)-**Bip**Pt(d(GpG)) conformer would be expected to be unfavorable, a conclusion consistent with the experimental evidence that no HT form has a significant abundance and only HH forms dominate. We conclude that the carrier ligand can have a major influence on conformer distribution in solution.

**New Rules for H8 Shifts.** The difficulty of assessing the position of the G bases by either coupling constants or NOE NMR data led Kozelka and Chottard to conduct a very enlightening and influential study employing computational methods to correlate conformational data from published X-ray and NMR structural investigations.[69] This 1992 article offered rules (K/C rules) for interpreting almost all the existing H8 shift data of *cis*-Pt($NH_3$)$_2$(d(GpG)) adducts in both single strands and

(67) Norman, D.; Abuaf, P.; Hingerty, B. E.; Live, D.; Grunberger, D.; Broyde, S.; Patel, D. J. *Biochemistry* **1989**, *28*, 7462−7476.

(68) Qu, Y.; Bloemink, M. J.; Reedijk, J.; Hambley, T. W.; Farrell, N. *J. Am. Chem. Soc.* **1996**, *118*, 9307−9313.

(69) Kozelka, J.; Fouchet, M. H.; Chottard, J.-C. *Eur. J. Biochem.* **1992**, *205*, 895−906.

duplexes. Furthermore, the rules were later used to interpret much of such oligonucleotide NMR shift data published subsequently.[43]

A full appreciation of the K/C rules requires that the reader consult the original article. For our discussion, we summarize relevant points here. A key aspect of the K/C analysis is that the *cis*-Pt($NH_3$)$_2$(d(GpG)) moiety is always the L variant in single strands, but it changes to the R variant in duplexes (Figure 2). An inductive effect (~0.4 ppm) causes all H8 signals to shift downfield relative to an uncoordinated G, giving a shift of ~8.5 ppm. This shift is modulated by the phosphate group on the 5′-G and by the ring current of the *cis*-G (calculated by using *cis*-Pt($NH_3$)$_2$(guanine)$_2$ as a model). For *cis*-Pt($NH_3$)$_2$-(d(GpG)) itself (L variant), the uncanted 3′-G base has an ~8.6 ppm H8 shift; this downfield position reflects the ring current deshielding by the *cis*-G (~0.1 ppm). The H8 shift for the canted 5′-G base is ~8.3 ppm; this upfield position is caused by the ring current shielding (~0.2 ppm) by the uncanted *cis*-G. In the K/C proposal, the 5′-phosphate on the 5′-G of *cis*-Pt($NH_3$)$_2$-(d(pGpG)) (L variant) does not affect the canting but has a nearly equal ~0.2 ppm downfield shifting effect on *both* H8 signals. For *cis*-Pt($NH_3$)$_2$(d(YpGpG), where Y contains at least one entire residue, the 5′-phosphate (attached to the 5′-G) is repositioned relative to Pt($NH_3$)$_2$(d(pGpG)) (Figure 2). The phosphate now affects mainly the H8 shift of the uncanted remote 3′-G (downfield H8 ~9 ppm). The H8 signal of the canted 5′-G is now farther upfield (~8 ppm). Compared to the typical single-strand species with a 5′ residue, the H8 shift in a duplex (R variant) is relatively less downfield (~8.7 ppm) for the uncanted G (now 5′) and is relatively less upfield (~8.2 ppm) for the canted G (now 3′).

We adapted these K/C rules to explain our recent NMR data on HT conformers of *cis*-Pt$A_2$**G**$_2$ retro models; in such complexes, the **G** bases are not linked, but dynamic motion is restricted by chiral bulky $A_2$ carrier ligands.[36,38,39,43,47] The rules were also useful to us in assessing the canting direction of **G** bases in HH conformers; for *cis*-Pt$A_2$**G**$_2$ models, such HH conformers have been found exclusively in retro models.

Despite the apparent wide applicability of the K/C rules, we have been puzzled for some time concerning the quantitative interpretation of H8 shifts of the HH form of our *cis*-Pt$A_2$**G**$_2$ retro models.[36,46,47] The K/C paper itself noted that, whereas the computations suggested that the L and R variants of *cis*-Pt($NH_3$)$_2$(d(GpG)) were similar in energy, the rules developed required that only the L variant dominated. Our **Bip**Pt(d(GpG)) complexes having different **Bip** chirality afford, for the first time, a closely related pair of HH1 isomers, one with an L and one with an R variant. *Results in Table 1 for these isomers cannot be understood with the K/C rules.*

We believe that the K/C rules fail to account for our new results both because the K/C analysis ignores the phosphate group linking the two G's and because the *cis*-Pt($NH_3$)$_2$(d(GpG)) moiety is assumed to be one variant in all cases. We offer *new* rules first and then justify these by explaining all existing data. In our rules, the H8 shifts for G's lacking a 5′-phosphate group are 8.7 (uncanted) and 7.8 ppm (canted). These values (which incorporate *cis*-G ring current effects) are based on our direct experimental measurements on **Bip**Pt(d(GpG)) conformers that exist mainly as one variant (Figure 6). Under our new rules, there is only the normal intraresidue 5′-phosphate effect, which shifts the H8 signal downfield by ~0.3 to ~0.4 ppm in the typical *anti* G residue; there is no remote interresidue effect. Consequently, the H8 shifts of G's bearing a 5′-phosphate group are 8.1−8.2 ppm and 9.0−9.1 ppm for canted and uncanted bases, respectively.

We compare the K/C analysis and our analysis first for the longer single-strand *cis*-Pt($NH_3$)$_2$(d(GpG)) adducts, since these seem to be mainly one variant, HH1 L (Figure 2). To explain the 3′-G H8 shift, which is typically very downfield (~9 ppm), the K/C analysis had to invoke an unusual, very large remote interresidue 5′-phosphate effect. Furthermore, the 5′-G H8 shift is typically upfield at ~8.1 ppm; the normal intraresidue 5′-phosphate effect would have to be very small. However, for the (*S,R,R,S*)-**Bip**Pt(d(GpG)) HH1 L variant, the 3′-G H8 shift of 9.1 ppm is also very downfield, *but there is no residue 5′ to the 5′-G* in (*S,R,R,S*)-**Bip**Pt(d(GpG)). Thus, the residue 5′ to the *cis*-Pt($NH_3$)$_2$(d(GpG)) cross-link in longer oligonucleotides does *not* have a through-space shifting effect as proposed in the K/C analysis. Rather, by our new rules, the characteristic downfield shift is a result of the lack of canting (normal shift ~8.7 ppm) and the 0.3-ppm deshielding effect of the phosphate between the cross-linked G's. The 5′-G in the HH1 (*S,R,R,S*)-**Bip**Pt(d(GpG)) conformer is fully canted, with a shift very close to the value of 7.8 ppm predicted by our rules for a residue lacking a 5′-phosphate. The H8 shifts of both the 5′-G and the 3′-G are exactly what is expected by our analysis if the longer oligonucleotides are >90% the HH1 L variant. (The equilibrium in Figure 2 lies to the left.) Thus, our analysis supports the K/C analysis in the conclusion that the HH1 L variant is favored for the *cis*-Pt($NH_3$)$_2$(d(GpG)) cross-link in longer single-strand oligonucleotides. However, we dismiss as unlikely the K/C proposal that the phosphate on the 5′-G has an unusual position, allowing the group to affect the 3′-G H8 shift.

Our analysis suggests that *cis*-Pt($NH_3$)$_2$(d(GpG)) is a dynamic mixture of various forms of comparable populations, in contrast to the longer adducts, which exist mainly as the HH1 L variant. Since a phosphate group has an effect on the G H8 shift when it is in the 5′ position, in a mixture of fluxional d(GpG) species the 3′-G H8 signal is likely to be downfield, as found in d(GpG) itself.[68] We calculate an average shift for the 3′-G H8 signal of *cis*-Pt($NH_3$)$_2$(d(GpG)) as 8.55−8.65 ppm [8.1−8.2 and 9.0−9.1, divided by 2] vs 8.57 ppm reported by K/C. For the H8 signal of the 5′-G (no 5′-phosphate), the average is 8.25 ppm vs the experimental value reported (8.27 ppm). This 5′-phosphate effect can account completely for the difference between the H8 shifts of *cis*-Pt($NH_3$)$_2$(d(GpG)). There is no need to invoke preferential canting of the 5′-G; its H8 signal is somewhat upfield because the 5′-G lacks a 5′-phosphate group. Put simply, canceling effects from dynamic mixture and the d(GpG) phosphate were both ignored in the K/C analysis of *cis*-Pt($NH_3$)$_2$-(d(GpG)).

The structure of *cis*-Pt($NH_3$)$_2$(d(pGpG)) has an equal population of HH1 R and HH1 L variants.[70] We believe that a mixture of variants also exists in solution. However, the K/C rules require that the HH1 L variant (5′-G canted) dominate. When HH1 conformational space was searched computationally in the K/C study, the 5′ terminal phosphate group was found to be positioned such that it could have an equal ~0.2 ppm downfield shifting effect on both H8 signals, accounting for the differences in shift of *cis*-Pt($NH_3$)$_2$(d(pGpG)) relative to that of *cis*-Pt($NH_3$)$_2$-(d(GpG)). However, our new rules indicate that the effect of the 5′-phosphate group is twofold: this group has a downfield shifting effect only on the 5′-G H8 signal and at the same time increases the population of the HH1 L variant (with a canted

(70) Sherman, S. E.; Gibson, D.; Wang, A. H. J.; Lippard, S. J. *J. Am. Chem. Soc.* **1988**, *110*, 7368−7381.

(71) Saenger, W. *Principles of Nucleic Acid Structure*; Springer-Verlag: New York, 1984; pp 1−556.

5′-G, Figure 2). Thus, compared to *cis*-Pt($NH_3$)$_2$(d(GpG)), the normal 5′-phosphate downfield shift effect on the 5′-G H8 shift is somewhat counteracted by an upfield shift due to the net increase in 5′-G canting, whereas the 3′-G H8 signal shifts downfield because the 3′-G base is in the less canted position more frequently. In summary, along the series *cis*-Pt($NH_3$)$_2$(d(GpG)) to *cis*-Pt($NH_3$)$_2$(d(pGpG)) to longer adducts, the percentage of the time that the base is canted increases for the 5′-G and decreases for the 3′-G. This new interpretation differs from that proposed in the K/C analysis.

**H8 Shifts for Non-HH1 Conformers.** For the *anti*,*syn* ΔHT1 (*S*,*R*,*R*,*S*)-**Bip**Pt(d(GpG)) conformer, the fully canted 5′-G (Figures 5 and 6) has an H8 shift (7.77 ppm) very close to the value of 7.8 ppm predicted by our rules based on HH1 conformers. The 3′-G is also canted. Furthermore, this residue has a *syn* conformation, diminishing the intraresidue phosphate effect so that the shift is similar to that of a canted G lacking a 5′-phosphate. The very unusual HH2 (*R*,*S*,*S*,*R*)-**Bip**Pt(d(GpG)) form deserves special mention. The canted bases (5′-G in HH1 and 3′-G in HH2) and uncanted bases (3′-G in HH1 and 5′-G in HH2) might be expected to have different shifts due to the phosphate effect. However, the H8 shifts of the canted bases are similar, as are the H8 shifts of the uncanted bases. Models show that, because the chain propagation direction in HH2 is opposite to normal, the phosphate is relatively closer to the 5′-G and farther from the 3′-G in the HH2 form than in the HH1 form. Thus, our new H8 shift analysis applies even to non-HH1 forms; these shifts *cannot* be explained with the previously accepted K/C rules.

**Summary and Implications.** Unique and unexpected results have arisen from our study of the reaction of the chiral enantiomers of [**Bip**Pt($H_2O$)$_2$]$^{2+}$ with d(GpG). We report here the first unambiguously identified HT atropisomer of a d(GpG) adduct with a single Pt. We believe that our studies of **Bip**Pt(d(GpG)) retro models have changed the landscape with regard to the underlying principles that have guided the interpretation of solution studies of guanine N7−Pt−N7 adducts, including *cis*-Pt($NH_3$)$_2$ adducts. Previously well-accepted interpretations of solution results do not apply to **Bip**Pt(d(GpG)) adducts. This finding led us to develop new interpretations of published data on *cis*-Pt($NH_3$)$_2$(d(GpG)), on *cis*-Pt($NH_3$)$_2$(d(pGpG)), and on longer oligonucleotides with a *cis*-Pt($NH_3$)$_2$(d(GpG)) cross-link. Ironically, our new analysis, based on solution results with adducts containing specially designed carrier ligands, allows us to rationalize computational, solution-state, and solid-state results on *cis*-Pt($NH_3$)$_2$(d(GpG)) adducts in a more consistent manner than do previous interpretations based on the *cis*-Pt($NH_3$)$_2$ adducts themselves. This success verifies the value of the retro-modeling approach.

Our study has a number of implications. The most obvious implication is that *cis*-Pt($NH_3$)$_2$(d(GpG)) is not only the HH1 L variant, as previously thought, but a mixture of forms. Also, the NMR shift analysis must also apply to duplex adducts. The *cis*-Pt($NH_3$)$_2$(d(GpG)) moiety is an R variant in duplexes; thus, the shift of the 3′-G H8 signal of ∼8.2 ppm is characteristic of a canted G affected by the d(GpG) phosphate. We believe that the structure of the cross-link within a duplex is most probably very close to that of the HH1 R variant reported for *cis*-Pt($NH_3$)$_2$(d(pGpG)) since this structure correctly positions the d(GpG) phosphate group so as to affect the 3′-G H8 shift.[70] The H8 shift (8.7 ppm) of the 5′-G in duplexes is remarkably invariant and is similar to the shift of an uncanted G lacking a 5′-phosphate group.[43] Our analysis indicates that this G is not canted.

The most important implication of our work is that lesions in DNA duplexes produced by less active Pt drug candidates with some carrier ligands may have high equilibrium percentages of HT or other conformers that differ from the HH1 R variant favored by *cis*-Pt($NH_3$)$_2$. Such lesions, which could also be kinetic products, may be more subject to repair than *cis*-Pt($NH_3$)$_2$ lesions. In most cases, not enough information is available to assess why a particular drug candidate was not as effective as *cis*-Pt($NH_3$)$_2$$Cl_2$. There is also usually no information to allow one to assess the conformation of adducts. However, our results shed some interesting light on one reported[3] drug candidate, **bmic**$PtCl_2$, which has moderate activity against P388 in a mouse model [**bmic** = (bis(*N*-methylimidazol-2-yl)-carbinol)]. The **bmic** carrier ligand lacks NH groups; lack of NH groups is a hallmark of low anticancer activity. Because the **bmic** carrier ligand is not $C_2$ symmetrical, **bmic**Pt(d(GpG)) can have *two* HH1 conformers; however, the authors of that study observed *five* distinct species by NMR spectroscopy. At the time the **bmic** paper was published in 1996, we had not reported our discoveries of the unprecedented HH2 and HT conformers. Thus, the authors utilized the prevailing concepts in the field and concluded that the five **bmic**Pt(d(GpG)) forms were all differently canted variants of one of the two HH1 conformers. We believe the barrier to wagging is too low for this to be the explanation, since the canted variants should interchange too rapidly to be distinguished by the NMR methods employed. Two of the five species had upfield $^{31}$P NMR signals; we believe that these two have an HT conformation. The other three forms have shifts indicative of HH conformers, and we suspect that one has the HH2 conformation.

On the basis of our results on the **Bip**Pt(d(GpG)) adducts and our reinterpretation of results on other N7−Pt−N7 d(GpG) cross-link adducts in the literature, it is now reasonable to advance the following new interrelated carrier ligand hypotheses: "The lower activity of cisplatin analogues is a consequence of non-HH1 conformers of N7−Pt−N7 d(GpG) cross-link DNA adducts. Non-HH1 conformers are more subject to repair than HH1 conformers. Non-HH1 conformers exist in dynamic equilibrium and at higher populations in adducts formed by analogues than in those formed by *cis*-Pt($NH_3$)$_2$$Cl_2$. The presence of NH groups on carrier ligands favors the HH1 conformer."

**Acknowledgment.** This work was supported by NIH Grant GM 29222 (to L.G.M.), MURST (Contribution 40%), CNR, and EC (COST Chemistry Project D8/0009/97 and D8/0012/97 (to G.N.)). We thank the Emory Microchemical Facility for MALDI-MS.

**Supporting Information Available:** NMR spectra and assignments of the mixed **Bip**Pt isomer reactions, rate constants determined from HPLC data, and molecular modeling structures (PDF). This material is available free of charge via the Internet at http://pubs.acs.org.

JA9916409